International Journal of Materials Chemistry and Physics
Vol. 1, No. 3, 2015, pp. 265-270
http://www.aiscience.org/journal/ijmcp

X-ray Diffraction Analysis of Polymeric Solid Using Bragg-Brentano Geometry

Biswajit Mallick*

Institute of Physics, Bhubaneswar, India

Abstract

The crystallographic structural parameters were analyzed using X'Pert-MPD XRD a laboratory X-ray source having Bragg-Brentano parafocusing optics. The line profile characteristics was obtained using *ProFit* -software based on Pseudo-Voigt profile function and is applicable for the study of interplaner spacing *d*, crystallite size D_{hkl}, percent crystallinity %C, macromolecular orientation and other structural imperfections of polyethylene terephthalate (PET). The polymeric solids possess very low intense diffraction peak as compared to metal because of its small amount of crystallinity and low Z constituents. Hence, it is quite difficult to record the whole diffraction pattern using a laboratory X-ray diffractometer. So far knowledge is concerned, there is no report on the observation of second order diffraction peaks from polymers using laboratory X-ray source. In the present report we have observed well resolved first order diffraction peaks with a signature of second order pattern from a polymeric solid applying a high-resolution diffraction geometry. The X-ray diffraction data obtained for solid PET matched well with the data reported by different researchers using high intense source like synchrotron.

Keywords

X-ray Diffraction, Bragg-Brentano, Profile Fitting, Polyethylene Terephthalate

Received: August 13, 2015 / Accepted: September 8, 2015 / Published online: September 25, 2015

1. Introduction

Among the advance polymer materials, polyethylene terephthalate (PET) is interesting because of its wide application in various fields due to its vast range of properties, which needs a wide range of methods of characterization. PET is significant because of its high mechanical strength, inertness to chemical action and resistance to thermal environment.

The first problem to be considered is that of the structure at the atomic level or 'fine structure' (molecular structure, crystal structure, distortion of the atomic arrangement, *i.e.*, crystalline / paracrystalline /amorphous, etc.). This involves the static arrangement of the atoms in the molecules from which the substance is formed. This, in turn, leads to an examination of the bonding relationship between atoms, the mutual orientations and contacts between the molecules. This kind of structural information gives valuable insights into the nature (*i.e.*, the physical and mechanical properties) of the substance. In general, crystalline high polymer [1] substances can be consisting of two phases, crystalline and amorphous. This concept is important for 'fine texture' (preferred orientation of crystalline regions, crystallinity, size and shape of crystalline regions, structure of amorphous regions, and arrangement of crystalline and amorphous state) and has a strong effect on the physical and mechanical properties of high polymers [1].

Solids in which there is no long-range order of the positions of atoms are called amorphous solids. Many polymeric solids are mainly found in amorphous state. Amorphous polymeric solids can exist in two different states, namely, the '*rubbery*' and the '*glassy*' state. In the melt, thermal energy is sufficiently high for long segments of each polymer-chain to move in random micro-Brownian motions [2]. As the melt is

* Corresponding author
E-mail address: bmallick@iopb.res.in

cooled, a temperature is reached at which all long-range segmental motion ceases or the transition between the glassy and rubbery states takes place. This temperature is called glass transition temperature or T_g. In the glassy state, at temperature below T_g, the only molecular motion that can occur is the short-range motion of several contiguous chain segments and the motion of substitute groups. These processes are called secondary relaxations.

However, polymers with regular long-range order of macromolecules are crystalline. The entire set of relaxation properties of a polymer manifests itself in the kinetics of crystallization and in the types of the crystalline structure [3]. Crystalline structure is featured by the participation of macromolecules folded on themselves so that the segments are oriented at right angles to the plane of the lamellas. The stress-strain curve and the laws of stress relaxation and creep for crystalline polymers have a definite analogy with their counterparts in glassy polymers. The distinction is due both to the differences in the mechanism deformation of crystalline and glassy polymers and to the appreciable content of an amorphous part in crystalline polymers, which increases deformability and lowers brittleness. When oriented polymers are produced, their strength and modulus increase, and their brittleness is lowered [3].

The X-ray analysis of polymer is often more difficult than the other classes of solids because of several reasons [1, 4, 5-16] *viz.* its difficulty in growing large crystals, intensity obtained is less and it falls off rapidly with diffraction angle (2θ) because of weak bonding, which leads to large temperature vibration coefficient, etc. The most important parameters in X-ray diffraction studies are intensity of the diffraction peak, interplaner distance (d) and full width at half maximum (*FWHM*). The above parameters can be accurately estimated by using sophisticated instruments and profile fitting program.

2. Experimental

An X'Pert-MPD PANalytical X-ray diffractometer (X'Pert-MPD, PANalytical, The Netherlands) with PW 3020 vertical goniometer having Bragg-Brentano parafocusing optics [13] and PW3710MPD control unit, has been used for the X-ray diffraction study. The geometry of Bragg-Brentano parafocusing optics as shown in Fig. 1 was employed for the high-resolution X-ray powder diffraction study. In the present system, there is a provision to get both line and point focus X-ray beam. CuK_α-radiation from a high power ceramic X-ray tube (operated at 40 kV and 40 mA) is initially collimated through Soller slit (texture collimator) of 0.04 rad, fixed divergence slit (0.25°-4°) and mask (2 - 20 mm) before getting it diffracted from the sample. Then the diffracted beam from the sample is well collimated by passing it through a programmable anti-scattering slit to reduce air scattering, programmable receiving slit and Soller slit (parallel plate) of 0.04 rad before getting it reflected by the Johann-type curved graphite crystal (002) of radius 225mm as post monochromator. An Xe-gas filled proportional counter (PW3011/10) of energy resolution 19% and maximum count rate of 750 kcps (with 2 cps background) is mounted on the arm of the goniometer circle at a radius of 200 mm to receive diffracted X-ray signal. Experimental control and data acquisition are fully automated through computer.

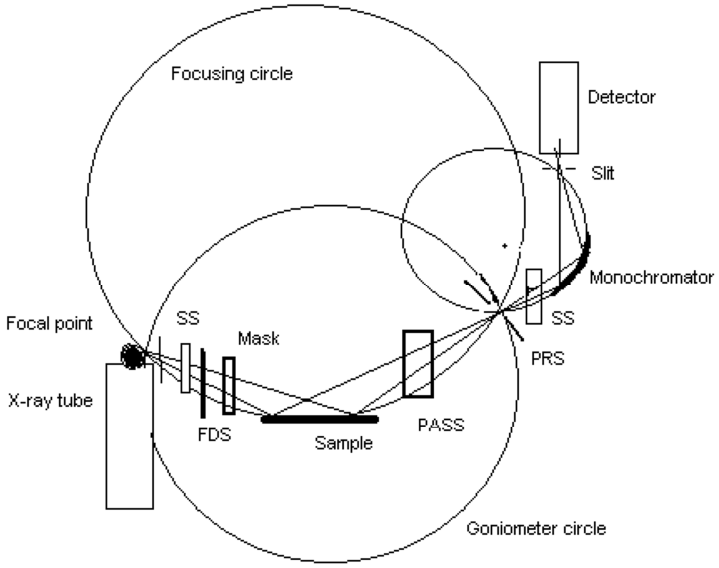

Fig. 1. Geometry of Bragg-Brentano parafocusing optics of X' Pert-MPD system. The abbreviations used are: SS for Solar slit, FDS for fixed divergence slit, PASS for programmable anti-scattering slit, PRS for programmable receiving slit. Radius of Goniometer (R_G), radius of focusing circle (R_F) and radius of monochromator (R_M) can be related as $R_F = [R_G / 2 \text{ Sin } \theta]$.

The X-ray fibre diffraction patterns were recorded with a step size of 0.01° on a 3°-55° range with a scanning rate of 0.0083°/sec. A line focus and collimated CuK_{α}-radiation from an X-ray tube operated at 40 kV and 30 mA was passed through fixed divergence slit of 0.5° and mask (10 mm) before getting it diffracted from the fibre sample. Then the diffracted beam from the sample was well collimated by passing it through a programmable anti-scattering slit of 0.5°, receiving slit of 0.15 mm and Soller slit before getting it reflected by the graphite monochromator. Experimental data such as *d* spacing, area of the diffraction peak and intensity were calculated using X'Pert Graphics & Identify software [13]. Also, the refined and fitted X-ray profile was calculated using *ProFit* software.

3. Analytical

The principles used for the measurements of the various structural parameters using X-ray diffraction are mainly based on the Bragg's law discussed below. If a monochromatic X-ray of wavelength λ is incident on a crystal of various sets of parallel equidistant planes at an angle θ_i, this gives rise to a reflected beam at an angle θ_r. Whether the two reflected rays will be in phase or out of phase will depend upon the path difference. When the path difference is equal to the wavelength or an integral multiple of the wavelength (*i.e.*, $n\lambda$), it produces diffraction pattern (which is called constructive interference). For more convenience, mathematically the above expression can be written as

$$2d_{hkl} \sin \theta_B = n\lambda \tag{1}$$

where θ_B (= θ_i) is the Bragg's angle or glancing angle, n (=1, 2, 3…) is the order of diffraction and d_{hkl} is the interplanar spacing of the crystal or particular material phase.

In general, the derivation [9] for all other simple lattices can be given as

$$n\lambda = \frac{2a_0}{\sqrt{F(hkl, abc, \alpha\beta\gamma)}} \sin\theta_B \tag{2}$$

where a b c are the unit lengths in x y z directions, α β γ are axial angles, and h k l are Miller indices of the planes, respectively.

Again, the intensity of diffracted beam depends on a number of factors. The amplitude and phase of the scattered wave are determined by arrangement of the atoms of the crystal relative to the plane in question. The structure factor for the centrosymmetric crystals has been expressed mathematically [11] as

$$F_{hkl} = \sum_{r=1}^{N} f_r \cos 2\pi(hx_r + ky_r + lz_r) \tag{3}$$

If the phase of the scattered beam is not known, we can write $|F_{hkl}|$ to represent its structure amplitude. A small phase difference between the diffracted waves from opposite sides of the atom results in a reduction of f_r, the scattering power of the atom, with increasing θ (scattering angle 2θ). When the scattering power of an atom is plotted against $\sin\theta / \lambda$ (usually called its *f*-curve), the value of *f* is equal to *Z*, the number of electrons in the atom (or ion), only when θ is zero.

The exact expression for the relative integrated intensity, *I* (arbitrary unit), of the powder line observed by diffractometer [12] is

$$I = |F_{hkl}| p \left(\frac{1+\cos^2 2\theta}{\sin^2\theta \cos\theta} \right) e^{-2M} \tag{4}$$

$$I = |F_{hkl}| \, p \, L_p \, e^{-2M} \tag{5}$$

where $|F_{hkl}|$ is the structure factor, p is the multiplicity factor, θ is the Bragg angle, e^{-2M} is the temperature factor and L_p is the Lorentz-polarization factor.

The profile shape was fitted to Pseudo-Voigt using *ProFit* [13] software and shown in Fig. 2(b). The profile-fitting program, *ProFit*, has been used to decompose a powder diffraction pattern into its constituent Bragg reflections by fitting analytical profile functions to obtain various parameters, which define the intensity, positions, breadth and shape of each reflection [14]. The software *ProFit* was developed to study crystallite size, microstrains and other structural imperfections. The line profile characteristics obtained can be used in other powder diffraction applications, such as identification of unknown phases, unit cell determination, indexing of powder patterns, quantitative analysis, structure refinement and *ab-inito* structure determination. The *ProFit* is mainly based on Pseudo-Voigt profile function *PV (x)*, which is defined as

$$PV(x) = I(x) = I_0[L(x) + G(x)] \tag{6}$$

where function x is the peak position, $L(x)$ and $G(x)$ are Lorentzian and Gaussian components respectively.

From above Eqn. (1), the Lorentzian (Cauchy) component is defined as

$$L(x) = \eta \frac{1}{1 + C_L(x - x_o)^2} \tag{7}$$

with $C_L = \eta \frac{1}{(w_L)^2}$

and the Gaussian component is defined as

$$G(x) = (1 - \eta).\, exp[-C_G (x - x_o)^2] \quad (8)$$

with $C_G = \eta \frac{ln\, 2}{(w_G)^2}$

where x_0 is the peak position, η is the mixing parameter, 2 w_L and 2 w_G are the *FWHM*'s of $L(x)$ and $G(x)$, respectively.

In the Pseudo-Voigt function, η is the "mixing parameter", which lies in the range $0 \le \eta \le 1$, and determines the shape of the profile, with pure Lorentzian (Cauchy) and pure Gaussian as the limiting cases.

4. Result and Discussion

A PET solid of 25 × 30 × 3 mm^3 was selected for X-ray diffraction study using PANalytical X' Pert MPD system. The X-ray diffraction profile obtained is shown in Fig. 2(a). The various important crystallographic parameters of the above solid obtained experimentally are recorded in Table-1. Again, a number of structural parameters have been calculated indirectly using the above diffraction data. The data obtained for solid PET matched well with the data obtained using high intense source like synchrotron [17].

Table 1. Structural study of solid PET.

2θ (deg.)	d (Å)	h k l	FWHM (deg.)	IR (%)	Peak height	Integrated Intensity A_{total}	Total area	Dhkl (Å)	Rmin
16.25	5.4501	0 -1 1	1.371	41.44	234	5292	5044	58.54	
17.61	5.0321	0 1 0	1.371	49.60	284	6408	6133	58.64	
21.53	4.1240	-1 1 1	1.371	50.32	214	4824	4587	59.00	0.091
22.81	3.8954	1 -1 0	1.371	74.07	425	9589	9253	59.12	
26.01	3.4229	1 0 0	1.371	100.0	585	13208	12813	59.48	
32.57	2.7469	1 1 1	1.371	7.97	61	1372	1247	60.37	

Again, the fitted profile was also refined by minimum-residual method. The minimum-residual method is capable of refining rough structure with greater degree of certainty than either the least-squares method or the method of steepest descents [15]. The correctness and the best fit of the X-ray structural data were determined by calculating the lowest value for the residual $R_{min,}$ using *ProFit* software, which can be defined as $R_{\min} = \frac{\sum\left[|F_o| - |F_c|\right]}{\sum |F_o|}$, where F_o and F_c are the observed and calculated structure factors, respectively. As a very rough rule of thumb, a value of 0.2-0.3 suggests that a structure is roughly corrected [11], but that the positions of at least some of the atoms need correcting; a value of less than 0.1 indicates that all the atoms are correctly placed and their parameters known with fair accuracy.

The profile fitting of solid PET is found to be satisfactory as the calculated R_{min} value is found to be 0.091 (the most appropriate value for the best fit is < 0.1). The crystallite dimension (D_{hkl}) of identified crystalline phase is calculated using corrected Scherrer formula [18, 19] as $D_{hkl} = \frac{K\lambda}{\beta' \cos\theta}$, where β' (= B - b) is the *FWHM* (full width at half maximum); B is the line width; b is the instrumental broadening; K is the shape factor (= 0.9); θ is the Bragg angle and λ is the wavelength of CuKα_1(1.54056 Å). The factor 57.3 is used to convert the value of β' from degree to radians to obtain D_{hkl} in angstrom unit (Å). However, the instrumental broadening [20] can be calculated as $b = \left[\frac{2\Delta\lambda}{\lambda}\tan\left(\frac{2\theta}{2}\right)\right] + \left[arc\,\tan\frac{W_R}{R_G}\right]$, where $\frac{\Delta\lambda}{\lambda}$ is the resolution of diffractometer (2.5×10^{-3}), θ is the Bragg (or glancing) angle, W_R is the receiving slit width (0.3 mm) and R_G is the radius of goniometer (200 mm). The smallest crystallite size $D_{0\text{-}11}$ observed is 58.54 Å. The highest crystallite size D_{111} was found out to be 60.37 Å at 2θ around 32.57º. Though, the second order diffraction peaks observed between 40º -60º (2θ) were not included in the calculation due to poor statistics. Again, the percent crystallinity (%C) was calculated using the expression as $\%C = (1 - \frac{A_{amor}}{A_{total}}) \times 100$, where A_{total} is the area under the diffraction curve. The percent crystallinity of polymeric solid sample was calculated to be 68.5%.

Structure of PET [21] is triclinic in nature having, a = 4.56 Å, b = 5.94 Å and c = 10.75 Å. The axial angles are: α = 98.5º, β = 118º and γ = 112º, with multiplicity 2 ($1\bar{1}$). Number of chains per unit cell (N_u) is 1 and molecular confirmation is near planar. The space group is $P\bar{1}$ (Herman Margin notation) or C_i' (Schoenflies notation). The crystal density is 1.455 g/cm^3. Its molecular weight of repeated unit (monomer) is 192 g/mole. Again, the azimuth angle (α), or

the average angle of macromolecule disorientation,of PET is defined in the substance composing the fibers in relation to the meridian or equator as $\alpha = \frac{K(2\theta_2 - 2\theta_1)}{2} = \frac{FWHM}{2}$, where K is the scale factor of diffraction pattern. Hence, the helix angle (α) of the polymer sample can be calculated by simplifying the relation obtained from uni-axial spiral orientation ($0^0 < \varphi < 90^0$) as $\varphi = \alpha \cos\theta$, where θ is the Bragg angle. Both azimuth and helix angle are found out to be very small with respect to the fiber axis. The spiral orientation φ, lies between 0.658° and 0.679° indicates the polymer possesses high molecular orientation.

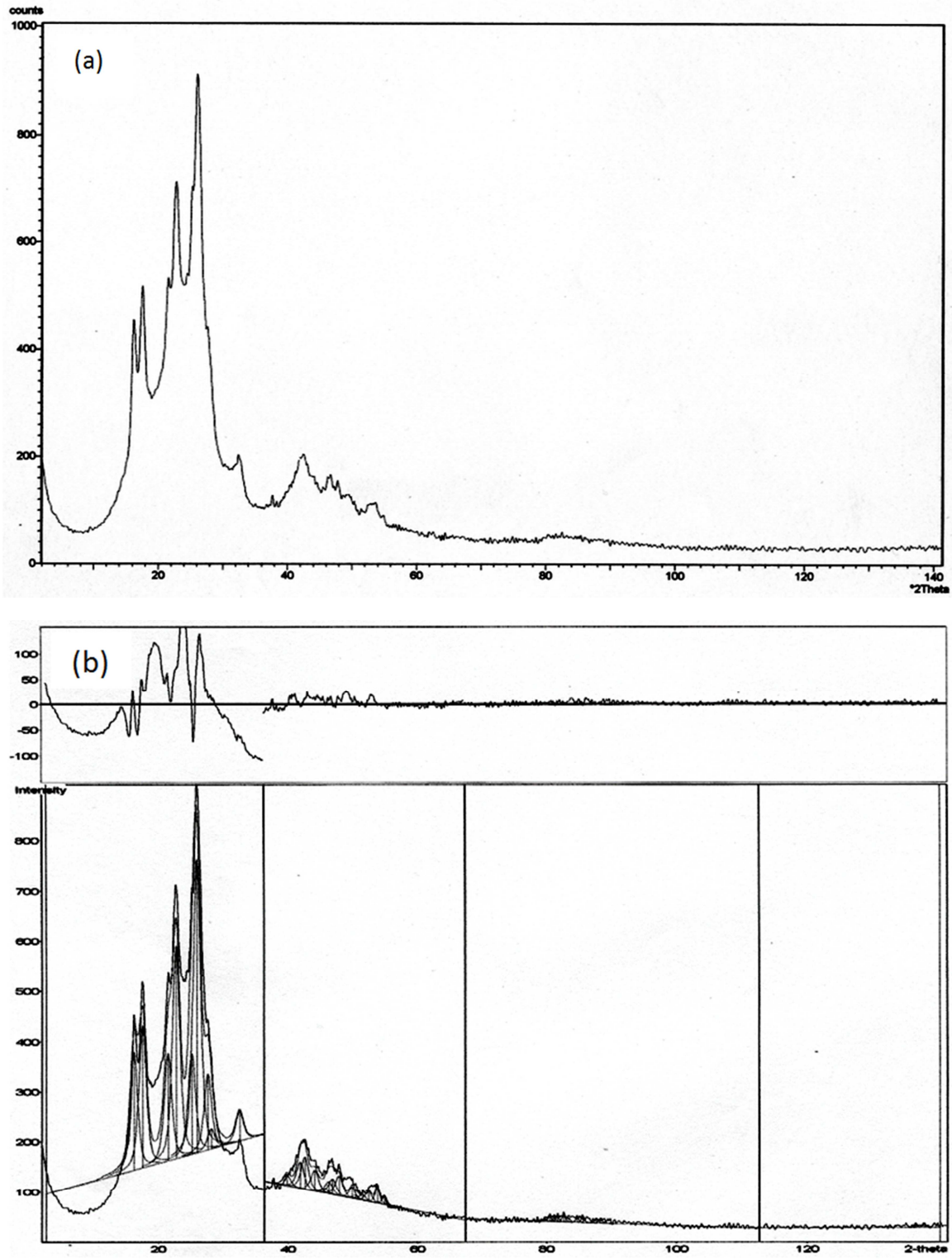

Fig. 2. (a) X-ray diffraction pattern of PET solid and (b) fitted X-ray diffraction profile of solid PET using *ProFit*.

5. Conclusion

X-ray investigation of PET solid was carried out using high-resolution diffraction geometry applying Bragg-Brentano parafocusing optics. The diffraction profile characteristics was obtained using *ProFit* software based on Pseudo-Voigt profile function. The structure of PET found out to be triclinic in nature with a = 4.56 Å, b = 5.94 Å and c = 10.75 Å. The plane (100) at $2\theta = 26.01^0$ was found to have the most intensity and maximum peak intensity I_{max}. The *d*-value of the 100% peak, i.e; I_{max} is found to be 3.4229 Å. Percent crystallinity %C of the polymeric solid was found to be 68.5%. Again, both azimuth and helix angles are found to be very small with respect to C-axis confirm the high molecular orientation. The particle size D_{hkl} lies between 58.54 Å to 60.37 Å. The X-ray diffraction data obtained for solid PET matched well with the data reported by others using high intense source like synchrotron. Hence, the present investigation will contribute greatly towards the study of polymer materials structure and to understand various crystallographic parameters of solids.

Acknowledgement

The author is indebted to Professor R C Behera Ex-Professor and Head, Department of Metallurgical and Materials Engineering and Professor S Panigrahi, Post-Graduate Department of Physics of National Institute of Technology, Rourkela, India for their valuable suggestions, help and encouragement during the study. In addition, the author is indebted to Professor T. N. Tiwari, Unique Research Centre, Rourkela, India for reading and spending his valuable time to correct the contents of manuscript.

References

[1] M. Kakudo, and N. Kasai, X-ray Diffraction by Polymers, Elsevier Publishing Company, Amsterdam, 1972.

[2] A. A. Vaiday, Production of Synthetic Fibres, Printice-Hall of India Pvt. Ltd., New Delhi, 1998.

[3] V. N. Kuleznev and V. A. Shershnev, The Chemistry and Physics of Polymers (Translated by G Leib) MIR Publishers, Moscow, 1990.

[4] G. L. Clark, The encyclopedia of X-ray and gamma ray, edited by G. L. Clark, Reinhold Publishing Corporation, New York, 1963.

[5] H. P. Klung and L. E. Alexander, X-Ray Diffraction Procedures for Polycrystalline and Amorphous Materials, John Wiley, New York, 1974.

[6] D. Campbell and J. R. White, Polymer Characterisation Physical Techniques, Champman & Hall, London, 1989.

[7] R. A. Fava, Polymers Part B: Crystal structure and Morphology, Academic Press New York, 1980.

[8] A. Guinier, X-Ray Diffraction in Crystals, Imperfect crystals, and Amorphous bodies, W.H. Free man & Company, London, 1963.

[9] A. Guinier and G. Fournet, Small-Angle Scattering of X-rays, (Translated by Walker C.B) John Wiley & Sons, Inc., New York, 1955.

[10] G. L. Clark, Applied X-rays, McGraw-Hill, New York, 1952.

[11] L. S. D. Glasser, Crystallography and its Applications, Van Nostrand Reinhold Company Ltd., New York, 1977.

[12] B. D. Cullity, Elements of X-ray Diffraction, Addision-Wesley Publishing Company, Inc., London, 1978.

[13] Philips Analytical X-ray, The Netherlands, *Pro Fit* software, 1999.

[14] J. I. Langford, D. Louer, E. J. Sonneveld and J. W. Visser, Powder Diffraction, vol. 1, 1986.

[15] H. Lipson and H. Steeple, Interpretation of X-ray Powder Diffraction Pattern, Macmillan, London, 1970.

[16] L. V. Azaroff, R. Kaplow, N. Kato, R. J. Weiss, A. J. C. Wilson and R. A. Young, X-Ray Diffraction, McGraw-Hill, New York, 1974.

[17] R. Gehrke, HASYLAB Summer student lecture: Small Angle X-ray Scattering, 2003.

[18] R. Jenkins and J. L. de Varies, Worked Examples in X-ray Analysis, The Macmillan Press Ltd., London, 1978.

[19] B. Mallick, T. Patel, R. C. Behera, S. N. Sarangi, S. N. Sahu, and R. K. Choudhury, Microstrain analysis of proton irradiated PET microfiber, Nucl. Instrum. Methods Phys. Res. B, 248 (2006) 305.

[20] T. Ida and K. Kimura, Flat-specimen effect as a convoluation in powder diffractometry with Bragg-Brentano geometry, J. Appl. Cryst. 32 (1999) 634.

[21] L. H. Sperling, Introduction to Physical Polymer Science, John Wiley & Sons, New York, 1986.